Examination of Some Commercial Sorptive Organobentonites

Müşerref ÖNAL

Ankara University, Faculty of Science, Department of Chemistry, Tandoğan, 06100 Ankara-TURKEY
e-mail: onal@science.ankara.edu.tr

For controlling organophilic partition nanophase (OPN) formation in some commercial sorptive organobentonites (OBs), 4 sample were selected randomly and examined by X-ray diffraction (XRD), Fourier transform infrared (FTIR) spectroscopy, differential thermal analysis (DTA), thermal gravimetric analysis (TGA), element analysis (EA), and nitrogen adsorption/desorption (N_2-AD) techniques. Since the d(001) values of the OB samples are between 1.94 and 3.36 nm, the pseudotrilayer or paraffin-type alkylammonium configuration located between the 2:1 layers of smectites is dominant. The bending and stretching type FTIR bands of the smectite surface and alkylammonium cations (AACs) are evidence of the formation of the OPN in the OBs. The DTA and TGA curves show that the thermal degradation of the intercalated AACs is completed between 250 and 550 °C as H_2O, CO_2, and charcoal are formed. The number of C atoms in the AACs used during the preparation of the OBs is between 30 and 42, according to EA. Oxidation of charcoal to CO_2 takes place between 550 and 800 °C. In the same temperature range, smectite is dehydroxylated to release H_2O. Decrystallization of smectite occurs near 1000 °C by an exothermic reaction and without any mass loss. It was observed that the intercalated AACs are flameproof at all temperature ranges applied. The shapes of the N_2 adsorption and desorption isotherms show that the OBs are mesoporous solids. The specific surface area (S) and specific mesopore volume (V) for each OB were determined by using the adsorption and desorption isotherms, respectively. The S and V values range between 33 and 50 m^2g^{-1}, and 0.095 and 0.191 cm^3g^{-1}, respectively. These values are virtually the same as those of natural bentonites. Since the S and V values do not approach zero, OPN formation in the commercial samples is far from completion.

Key Words: Infrared spectra, organobentonites, porosity, surface area, thermal analysis, X-ray diffraction.

Introduction

Bentonites and their major clay mineral, smectites, are known to be efficient gellants for water systems, but they do not gel effectively in organic liquids.[1−3] It has been observed that a bentonite with high swelling properties in water showed a tendency to swell in various organic liquids after reacting with some organic ammonium salts.[4,5]

An organophilic clay obtained by the exchange of interlayer inorganic cations with organic cations is called an organobentonite (OB).[6-8] An OB may be also be called an organoclay, organosmectite, or organomontmorillonite. In the present study the term OB was preferred. Natural exchangeable metal cations, such as Na^+ and Ca^{2+}, located between the 2:1 layers of smectite, are released into solution by the formation of OBs. The intercalated organic cations act as pillars to hold the 2:1 layers permanently apart.[9-13]

Several investigations have been conducted since OBs were first prepared.[4] The surface properties of bentonites were modified greatly by replacing natural inorganic exchangeable metal cations with larger alkylammonium, alkyldiammonium, and quaternary ammonium cations of the forms $[CH_3 (CH_2)_n NH_3]^+$, $[NH_3 (CH_2)_n NH_3]^{2+}$, and $[(CH_3)_3 NR]^+$ or $[(CH_3)_2 NRR']^+$, respectively.[14-18] Here, R and R' are non-polar alkyl groups with more than 12 C atoms. They may also contain aromatic rings. If R and R' are small, with less than 12 C atoms, such as CH_3-, CH_3-$(CH_2)_{10}-$, or simply phenyl groups, such materials are classified as adsorptive OBs. When they are large, with 12 or more C atoms, such materials are classified as organophilic or sorptive OBs. Large cations, such as hexadecyltrimethylammonium, dodecyltrimethylammonium, and octadecyltrimethylammonium, are generally used in the production of sorptive OBs.[19-21] The large alkyl groups of these cations form a continuum of the organophilic partition nanophase (OPN) in the interlayers of smectites.[22] This OPN functions as a partition medium for non-polar organic compounds and is highly effective in removing such organic compounds from waste water.[23,24] The sorption process of the OPN appears mechanistically similar to the dissolution of neutral organic compounds in a bulk organic-solvent phase, such as hexane or octane.[25-27] Several studies have been carried out on the sorption of alkanes, aliphatic alcohols, herbicides, insecticides, fungicides, and many other organic pollutants on sorptive organobentonites.[28-32]

The interlayer of a natural smectite continuously opens up with the progress of OPN formation, depending on the size and orientation of the intercalated alkylammonium cations (AACs). This phenomenon was examined by X-ray diffraction (XRD), Fourier transform infrared spectroscopy (FTIR), differential thermal analysis (DTA), thermal gravimetric analysis (TGA), and nitrogen adsorption/desorption techniques (N_2-AD).[33-38] The change in adsorptive properties, including specific surface area (S) and specific micromesopore volume (V), of a bentonite by intercalation can be determined by N_2-AD. Nitrogen adsorption data have the potential to be employed in identifying OPN formation. It has been known for a long time that AACs do not only occupy the 2:1 interlayers, but also the edges, which means a partial closure of the pore openings.[39,40] Therefore, the S and V values decrease as OPN formation progresses, and reaches zero when the formation is complete. Based on this fact, XRD, FTIR, DTA, and TG studies can be supported by the measurement of S and V values in determining the progress of OPN formation. The purpose of the present study was to examine some commercial sorptive OBs based on the progression of OPN formation.

Materials and Methods

The study used 4 randomly selected commercial sorptive OBs. The first 3, Bentone SD-1, Bentone SD-2, and Bentone 34, were supplied by Rehox (Bayer Chemie, BASF), and the fourth, Viscobent SB-1, is produced by Bensan (Enez, Turkey). They are generally used as rheological additives. The XRD patterns of the organobentonites were obtained from random mounts using a Rikagu D-Max 2200 powder diffractometer with CuK_α radiation and a Ni filter. The FTIR spectra of the samples were determined with a Mattson 1000 FTIR spectrophotometer in the wavenumber interval, 400-4000 cm^{-1}, using the KBr disk procedure. The DTA and TGA curves of the samples were determined with a Netzch Model 429 instrument at a heating

rate of 10 K min^{-1} and α-Al$_2$O$_3$ was used as the inert reference. The carbon and nitrogen contents of the air dried OBs were determined with an element-analyzer (LECO CHNS 932). The isotherms of the adsorption and desorption of nitrogen in the samples at liquid nitrogen temperature were determined by a volumetric adsorption instrument. The instrument was connected to strong vacuum made of Pyrex glass.[41]

Results and Discussion

Basal spacings

The XRD patterns of the organobentonites are given in Figure 1. Basal spacing, d(001), represents the 2:1 (TOT) layer thickness of smectites. The d(001) values of the sodium smectite (NaS) and calcium smectite (CaS) are approximately 1.20 nm and 1.55 nm, respectively. OBs have been generally prepared using natural NaS. The basal spacings of the investigated OBs are represented in Figure 1. The d(001) values scattered around 1.00 nm are considered evidence of illite impurities in the natural smectites used for the preparation of the OBs. Anhydrous smectites also have the same basal spacing. The d(001) values between 1.20 and 1.40 nm are due to the monolayer alkylammonium configuration in the interlayer space of the expanding 2:1 layers. The d(001) values between 1.40 and 1.80 nm are due to the bilayer alkylammonium configuration in the 2:1 layers. The d(001) values > 1.80 nm are due to the pseudotrilayer or paraffin-type alkylammonium configurations in the 2:1 layers.[26] The intensities of the 001 peaks show that the dominant configuration is the pseudotrilayer or paraffin-type.
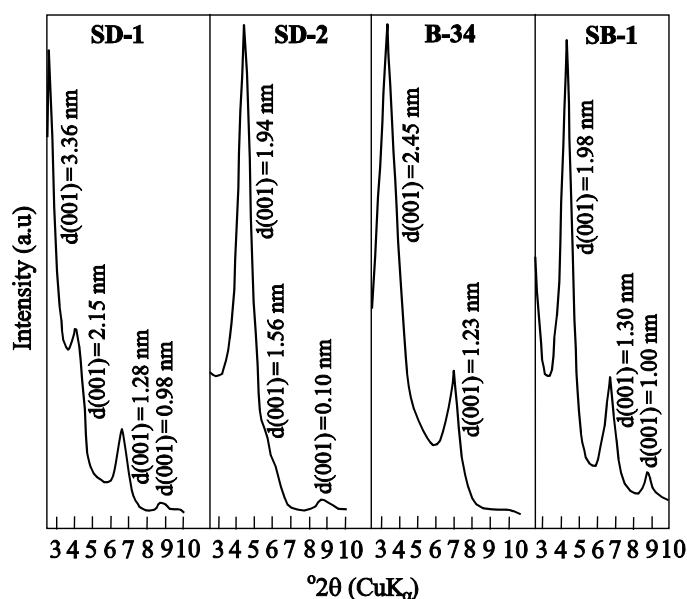
Figure 1. XRD patterns of the OBs.

FTIR spectra

Figure 2 shows the FTIR spectra of the OBs. The bands of the spectra at the lower wavenumber region are due to the bending vibrations, whereas those at the high wavenumber region are due to the stretching vibrations of the bonds.[42−46] The positions and assignments of the bands are given in Figure 2. The

bands near 470, 524, and 1036 cm^{-1} are assigned to the Si-O-Si, Al-O-Si, and Si-O bending vibrations, respectively.[47] The bands at 1634 and 3632 cm^{-1} are assigned to the hydroxyl bending vibrations of water and stretching vibration of the structural hydroxyl group of smectites, respectively. The bands at 1452 cm^{-1} correspond to the bending vibration of the C-H bonds found in all of the AACs. The bands near 2850 and 2960 cm^{-1} are characteristic of the stretching vibrations of the C-H bonds in the intercalated AACs. The band at 3365 cm^{-1} belongs to the stretching vibration of the H-OH bonds located in water molecule cations. In addition to the structural smectite bands, the bands belonging to the AACs are evidence of the formation of OBs.
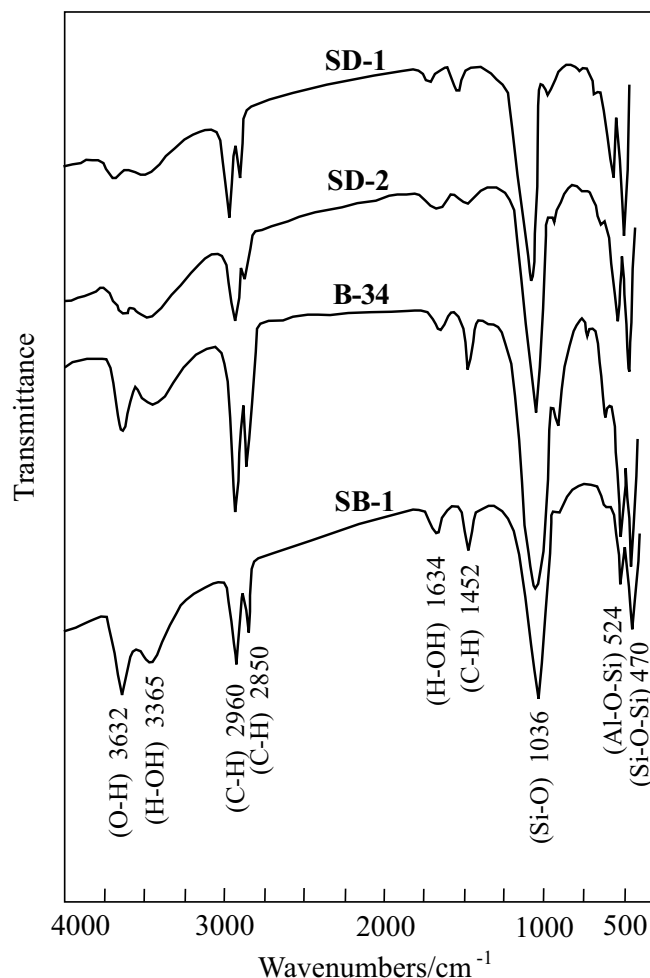
Figure 2. FTIR spectra of the OBs.

Thermal analysis

Thermal analysis, in combination with other methods, such as X-ray diffraction and IR spectroscopy, is suitable for the characterization of OBs.[48−51] The DTA and TGA curves of the OBs are given in Figure 3 and Figure 4, respectively, for the temperature range 25-1100 °C. The DTA curves show 3 endothermic and 2 exothermic changes. The maximum rate of temperature change is shown in the TGA curves. All mass losses and corresponding temperature intervals are represented on the TGA curves seen in Figure 4. The changes were evaluated in light of the literature,[52] as described below.
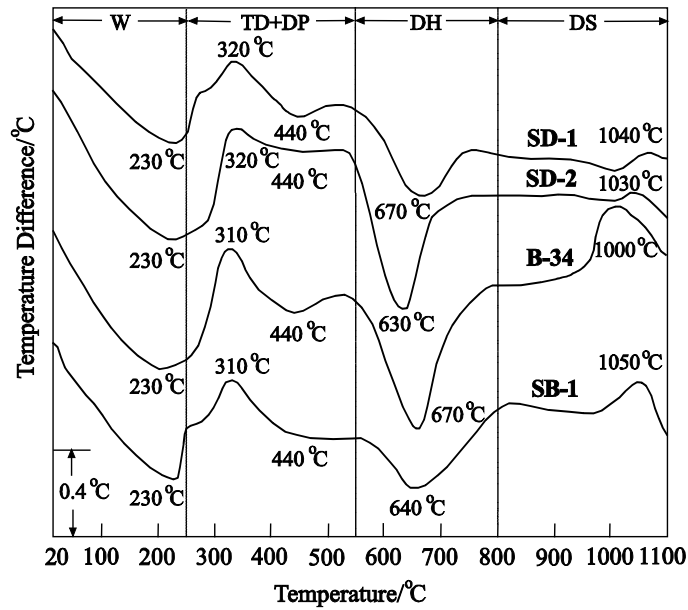
Figure 3. DTA curves of the OBs (W: interparticle water; TD: thermal degradation; DP: degradation products; DH: dehydroxylation; DS: decrystallization of smectite).
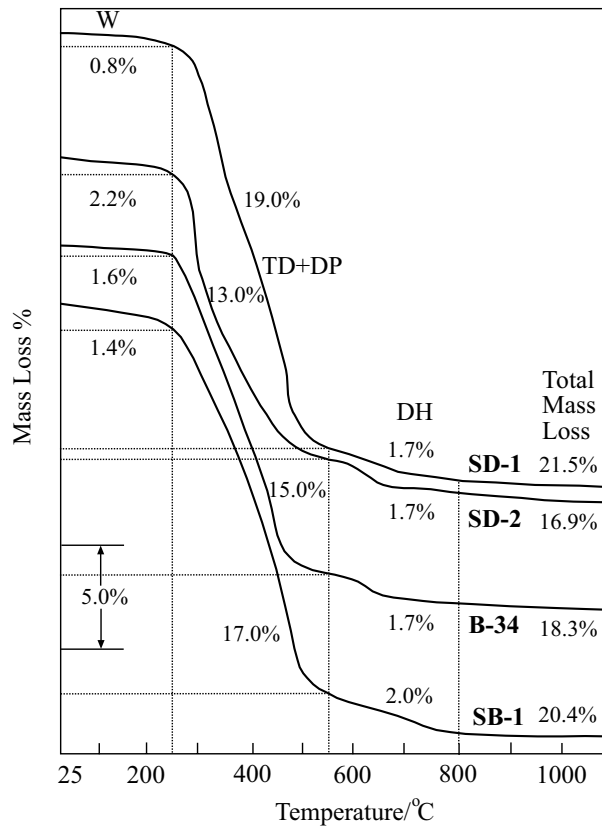
Figure 4. TGA curves of the OBs (W: interparticle water; TD: thermal degradation; DP: degradation products; DH: dehydroxylation; DS: decrystallization of smectite).

The first endothermic change at 25-250 °C, with a maximum rate at around 230 °C, is due to the dehydration of interparticle water or adsorbed water (W), known as moisture. The moisture content of the OBs is seen in the TGA curves between 0.8% and 2.2% by mass. The first exothermic change at 250-550 °C, with a maximum rate at around 310 °C, is assigned to the thermal degradation (TD) of intercalated AACs to H_2O, CO_2, and charcoal. The mass loss due to TD ranges between 13% and 19%, depending on the OBs. The second endothermic change at 550-800 °C, with a maximum rate at around 650 °C, is due to the oxidation of the remaining charcoal and dehydroxylation (DH) of smectites. The mass losses due to this stage range between 1.7% and 2.0%. The second exothermic change, without mass loss between 950 and 1100 °C, is due to the decrystallization of smectites (DS). The total mass loss in SD-1, SD-2, B-34, and SB-1 by heating up to 1100 °C was 21.5%, 16.9%, 18.3%, and 20.4%, respectively.

Element analysis

The percentage of C and N by mass, as well as the molar ratio of C/N of the OBs are given in the Table. Because there is only one N atom in the AACs, the molar C/N ratio also gives the number of C atoms in such cations. The AACs used for the preparation of the sorptive OBs are generally tetraalkylammonium (quaternary) cations with the formula $[R_1\ R_2\ R_3\ R_4N]^+$, where R_s are the alkyl groups. These groups may be the same or different. The interlayer space of the OBs increases as the number of C atoms in the R groups increases. For our samples, the change in basal spacing, as a function of the number of C atoms, is given in Figure 5. In addition to the number of C atoms, the change in the d(001) value is dependent on the size and orientation of the R group. For this reason, the d(001) value displays a sudden jump when the number of C atoms increases from 35 to 36.
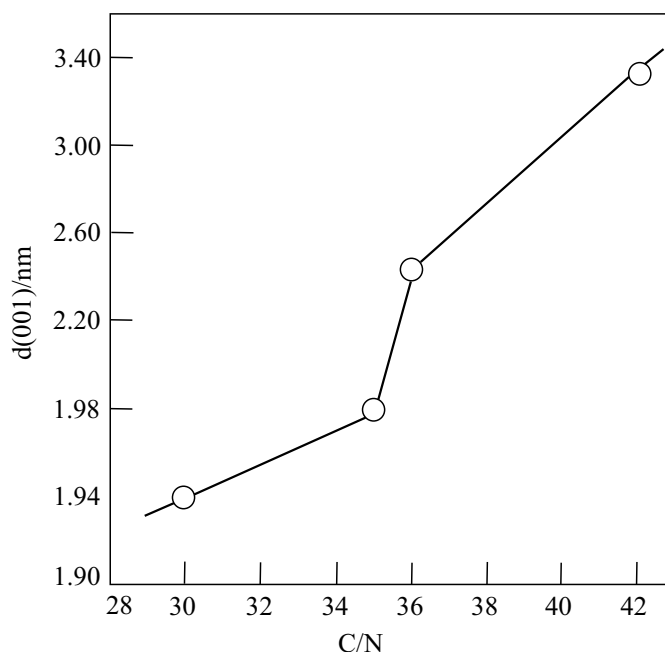
Figure 5. The change in the basal spacing of the C/N molar ratio.

Table. Basal spacing, the carbon and nitrogen content (%), C/N molar ratio, specific surface area, and specific mesopore volume of the examined sorptive OBs.

OBs	d(001)/nm	C %	N %	C/N	A/m^{2}g^{-1}	V/cm^{3}g^{-1}
Bentone SD-1	3.36	37.23	1.04	42	50	0.095
Bentone SD-2	1.94	29.34	1.15	30	52	0.191
Bentone B-34	2.45	28.88	0.93	36	33	0.102
Viscobent SB-1	1.98	32.52	1.08	35	43	0.120

Adsorptive properties

The nitrogen adsorption and desorption isotherms at the liquid nitrogen temperature for the OBs were drawn, and a representative plot for the Viscobent SB-1 is shown in Figure 6. Here, p is the adsorption equilibrium pressure, p° is the vapor pressure of bulk liquid nitrogen at the experimental temperature, p/p° $\equiv$ x is the normalized adsorption equilibrium pressure, and n is the adsorption capacity defined as the molar amount of nitrogen adsorbed by 1 g of adsorbent at any x. According to the Brunauer classification, these isotherms are similar to type II[53]. The shapes of the isotherms indicate that the OBs mainly have mesopores with a radius between 1 and 25 nm. The micropores with a radius < 1 nm in the OBs are negligible compared to the mesopores. After completion of monomolecular and multi-molecular adsorption up to x = 0.35, capillary condensation begins and mesopores reach x = 0.96. Bulk liquid nitrogen forms at x = 1.[54] Capillary condensed nitrogen in mesopores, due to adsorption, also undergoes capillary evaporation by desorption at the interval 0.96 > x > 0.35. The desorption isotherm does not overlap with the corresponding adsorption isotherm at the interval 0.35 > x > 0. This shows that the multi-molecular and monomolecular adsorptions are not exactly reversible. The irreversibility is due to the hindrance of the diffusion of desorbed nitrogen molecules from the partition phase located in the interlayer of smectite.
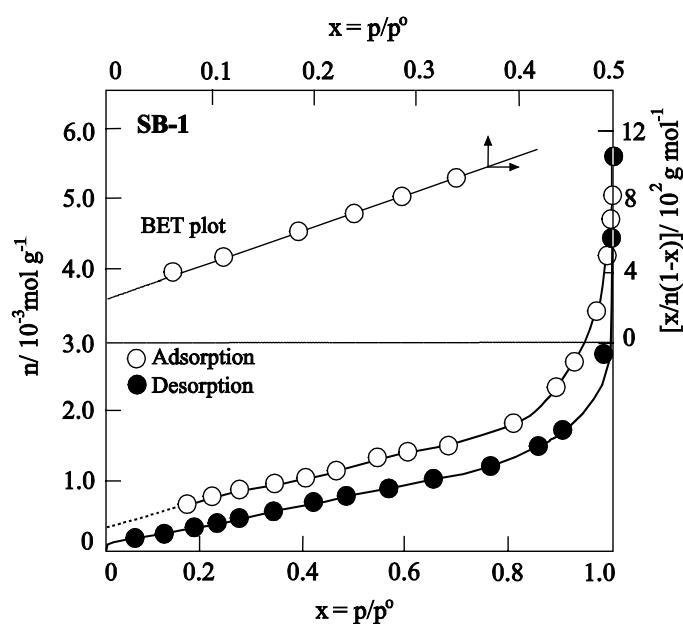
Figure 6. The adsorption-desorption isotherms and BET plot of OBs SB-1.

The specific surface areas (S/m^2g^{-1}) were obtained by the well-known standard Brunauer, Emmett, and Teller (BET) procedure, using adsorption data at the interval $0.05 < x < 0.35$.[55−58] A representative BET plot for Viscobent SB-1 is seen in Figure 6. The S values are given in the Table. The adsorption capacities, as liquid nitrogen volumes estimated from desorption isotherms at $x = 0.96$, are taken as the specific micro-mesopore volumes (V/cm^3g^{-1}) of the powders.[58] The V values are given in the Table. The S and V values of the natural bentonites, depending on their geological formation, mineralogy, and chemical composition, are between 20 and 80 m^2g^{-1} and 0.08-0.30 cm^3g^{-1}, respectively. The S and V values of the investigated OBs are not far from those of natural bentonites. This is evidence of the partial formation of OPN in the OBs.

Conclusion

In addition to XRD, FTIR, DTA, TGA, and EA findings, low temperature adsorption/desorption data were used to comment on the type and progress of OB formation. Increases in the surface area and porosity of the OBs indicate that new micro- and mesopores are formed. Conversely, decreases in these properties signal the closing of those pores. This behavior is attributed to the OPN and sorptive OB formation. Furthermore, a sharp decrease in the surface area and porosity shows the complete formation of the OPN in the OBs. Low temperature N_2 adsorption data were shown to be useful in determining and discussing the S and V values. Based on this result, determining if OPN has partially or completely formed should include the evaluation of low temperature adsorption results.

Acknowledgment

References

1. R.E. Grim, **"Clay Mineralogy",** McGraw-Hill, New York**,** 1968.

2. R.E. Grim, and N. Güven, **"Bentonites-Geology, Mineralogy, Properties and Uses (Developments in Sedimentology, 24)",** Elsevier, New York, 1978.

3. H.H. Murray, **Appl. Clay Sci. 17,** 207-221 (2000).

4. J.W. Jordon, **J. Phys. Chem. 53,** 294-306 (1949).

5. J.W. Jordon, B.J. Hook and C.M. Finlayson **J. Phys. Chem. 54,** 1196-1208 (1950).

6. M.M. Mortland, **Adv. Agron. 22,** 75-117 (1970).

7. B.K.G. Theng, **"The Chemistry of Clay Organic Reactions",** Adam Hilgar, London, 1974.

8. G. Lagaly, **Philos. T. Roy. Soc. A311**, 315-332 (1984).

9. M.S. Whittingham and A.J. Jacobson, **"Intercalation Chemistry",** Academic Press, New York, 1982.

10. M. Iwasaki, M. Kita, K. Ito, A. Kohno and K. Fukunishi, **Clays Clay Miner. 48,** 392-399 (2000).

11. N. Khaorapapong, K. Kuroda and M. Ogawa, **Clays Clay Miner. 50,** 428-438 (2002).

12. M. Ogawa, T. Ishii, N. Miyamoto and K. Kuroda, **Appl. Clay Sci. 22,** 179-185 (2003).

13. V. Luptáková and G. Plesch, **Clay Miner. 40,** 295-302 (2005).

14. R.M. Barrer and D.M. MacLeod, **Trans. Faraday Soc. 50,** 980-989 (1954).

15. R.M. Barrer and D.M. MacLeod, **Trans. Faraday Soc. 51,** 1290-1300 (1955).

16. Z. Zhang, D.L. Sparks and N.C. Scrivner, **Environ. Sci. Technol. 27,** 1625-1631 (1993).

17. K.A. Carrado, P. Thiyagarajan and K. Song, **Clay Miner. 32,** 29-40 (1997).

18. T. Polubesova, G. Rytwo, S. Nir, C. Serban, and L. Margulies, **Clays Clay Miner. 45,** 834-841 (1997).

19. Z. Klapyta, T. Fujita and N. Iyi, **Appl. Clay. Sci. 19,** 5-10 (2001).

20. S.Y. Lee and S.J. Kim, **Clays Clay Miner. 50,** 435-445 (2002).

21. J.K. Bonczek, W.G. Harris and P. Nkedi-Kizza, **Clays Clay Miner. 50,** 11-17 (2002).

22. K-W. Park, S-Y. Jeong and O-Y. Kwon, **Appl. Clay Sci. 27,** 21-27 (2004).

23. C.T. Chiou, D.W. Schmedding and M. Manes, **Environ. Sci. Technol. 16,** 4-10 (1982).

24. C.T. Chiou, P.E. Porter and D.W. Schmedding, **Environ. Sci. Techol. 18,** 295-297 (1983).

25. S.A. Boyd, M.M. Mortland and C.T. Chiou, **Soil Sci. Soc. Am. J. 52,** 652-657 (1988).

26. A.R. Mermut, **"Layer Charge Characteristics of 2:1 Silicate Clay Minerals"** The Clay Minerals Society, Aurora, CO, USA, 1994.

27. B.L. Sahney, **"Organic Pollution in the Environment"** The Clay Minerals Society, Aurora, CO, USA, 1996.

28. R.M. Barrer, **Pure Appl. Chem. 61,** 1903-1912 (1989).

29. M. Harper and C.J. Purnell, **Environ. Sci. Technol. 24,** 55-62 (1990).

30. L. Zhu and Y. Su, **Clays Clay Miner. 50,** 421-427 (2002).

31. M.J. Carrizosa, W.C. Koskinen, M.C. Hermosin and J. Cornejo, **Soil Sci. Soc. Am. J. 67,** 511-517 (2003).

32. T. Ocada, T. Morita and M. Ogawa, **Appl. Clay. Sci. 29,** 45-53 (2005).

33. S. Yariv, **Appl. Clay Sci. 24,** 225-236 (2004).

34. S. Yariv and I. Lapides, **J. Ther. Anal. Cal. 80,** 11-26 (2005).

35. Y. Xi, Z. Ding, H. He and R.L. Frost, **J. Colloid Interf. Sci. 277,** 116-120 (2004).

36. Y. Xi, W. Martens, H. He and R.L. Frost, **J. Ther. Anal. Cal. 81,** 91-97 (2005).

37. D. Ovadyahu, I. Lapides and S. Yariv, **J. Ther. Anal. Cal. 87,** 125-134 (2007).

38. H. He, Q. Zhou, W. N. Martens, T.J. Kloprogge, P. Yuan, Y. Xi, J. Zhu and R.L. Frost, **Clays Clay Miner. 54,** 689-698 (2006).

39. H. He, Z. Ding, J. Zhu, P. Yuan, Y. Xi, D. Yang and R.L. Frost, **Clays Clay Miner. 53,** 387-393 (2005).

40. M. Önal and Y. Sarıkaya, **Colloid Surface A: Physicochem. Eng. Aspects 296,** 216-221 (2006).

41. Y. Sarıkaya and S. Aybar, **Commun. Fac. Sci. Uni. Ank. 24B,** 33-39 (1978).

42. V.C. Farmer and J.D. Russell, **Spectrochim. Acta B 20,** 1149-1173 (1964).

43. V.C. Farmer, **"The Infrared Spectra of Minerals"** Monograph 4. Mineralogical Society, London, 1974.

44. R.M. Silverstein, G.C. Bassler and T.C. Morrill, **"Spectrophotometric Identification of Organic Compounds"** John Wiley and Sons, New York, 1981.

45. P.R. Griffiths and J.A. Haseth, **"Fourier Transform Infrared Spectroscopy"** John Wiley and Sons, New York, 1986.

46. B. Stuart, **"Modern Infrared Spectroscopy"** John Wiley and Sons, New York and Chichester, UK, 1996.

47. P. Komadel, **Clay Miner. 38,** 127-138 (2003).

48. S. Yariv, **"Differential Thermal Analysis (DTA) of Organo-Clay Complexes"** In: Eds. W. Smykatz-Kloss, S.St. J. Warne, Thermal Analysis in Geosciences. Springer Verlag, Berlin, 1991.

49. V. Balek, Z. Malek, U. Ehrilcher, K. Györyová, G. Matuschek and S. Yariv, **Appl. Clay Sci. 21,** 295-302 (2002).

50. S.M. Koh, M.S. Song and T. Takagi, **Clay Miner. 40,** 213-222 (2005).

51. F. Kooli and C.M.M. Magusin, **Clay Miner. 40,** 233-243 (2005).

52. V. Hlavaty and V.S. Fajnar, **J. Therm. Anal. Cal. 67,** 113-118 (2002).

53. S. Brunauer, L.S. Deming, D.M. Deming and E. Teller, **J. Am. Chem. Soc. 62**, 1723-32 (1940).

54. B.G. Linsen, **"Physical and Chemical Aspects of Adsorbents and Catalysts"** Academic Press, London, 1970.

55. S. Brunauer, P.H. Emmett and E. Teller, **J. Am. Chem. Soc. 60,** 308-319 (1938).

56. A.L. McCellan and H.F. Honsberger, **J. Colloid Interf. Sci. 23,** 577-599 (1967).

57. D.H. Everett, G.D. Parfitt, K.S.W. Sing and R. Wilson, **J. Appl. Chem. Biotechnol. 24,** 199-219 (1974).

58. F. Rouquerol, J. Rouquerol and K. Sing, **"Adsorption by Powder and Porous Solids",** Academic Press, London, 1999.